

Investigation of thermal and magnetic properties of defects in a spin-gap compound NaV_2O_5

A. I. Smirnov, S. S. Sosin

P. L. Kapitza Institute for Physical Problems RAS, 117334 Moscow, Russia

R. Calemczuk

Centre d'Etudes Atomique, Grenoble, Cedex 9 France

V. Villar, C. Paulsen

Centre Nationale de Recherches Scientifique, Grenoble, Cedex 9 France

M. Isobe, Y. Ueda

Institute for Solid State Physics, University of Tokyo, 7-22-1 Roppongi, Minato-ku, Tokyo 106, Japan

(November 2, 2018)

The specific heat, magnetic susceptibility and ESR signals of a Na-deficient vanadate $\text{Na}_x\text{V}_2\text{O}_5$ ($x=1.00 - 0.90$) were studied in the temperature range 0.07 - 10 K, well below the transition point to a spin-gap state. The contribution of defects provided by sodium vacancies to the specific heat was observed. It has a low temperature part which does not tend to zero till at least 0.3 K and a high temperature power-like tail appears above 2 K. Such dependence may correspond to the existence of local modes and correlations between defects in V-O layers. The magnetic measurements and ESR data reveal $S=1/2$ degrees of freedom for the defects, with their effective number increasing in temperature and under magnetic field. The latter results in the nonsaturating magnetization at low temperature. No long-range magnetic ordering in the system of defects was found. A model for the defects based on electron jumps near vacancies is proposed to explain the observed effects. The concept of a frustrated two-dimensional correlated magnet induced by the defects is considered to be responsible for the absence of magnetic ordering.

PACS numbers: 75.10.Jm, 75.40.Cx, 75.50.Ee, 75.45.+j, 76.30.-v

I. INTRODUCTION

The sodium vanadate NaV_2O_5 is a unique compound with 1D-magnetic structure formed within V-O layers due to the special arrangement of vanadium-oxygen orbitals. An intensive study of this compound began when a phase transition into a dimerized spin state was discovered¹. According to the present model, vanadium-oxygen bonds give rise to a ladder structure with one electron (and one spin) per rung which should be shared between two vanadium ions²⁻⁵. Electrons are localized at rungs due to the Coulomb repulsion in accordance with the dielectric state of the crystal. In the high temperature phase the average charge of each vanadium ion is +4.5. The phase transition into a spin-gap state at $T=36$ K was at first interpreted as a spin-Peierls transition¹. Further theoretical and experimental investigations⁶⁻⁸ point to a charge ordering phase transition that results in a zigzag charge distribution along the ladders, with a doubling of the lattice period and with alternating exchange interactions. The latter is responsible for the spin-gap opening according to Ref. 9. The spin-gap causes an exponential freezing of the spin part of the magnetic susceptibility observed below the transition¹⁰.

There are two reasons why the problem of defects in the spin-gap crystals is of great interest. First, soliton-type spin clusters may be formed around imperfect spins or

nonmagnetic impurities¹¹⁻¹³. These clusters are mesoscopic multispin objects with a microscopic total spin. The multispin nature of such clusters was confirmed by ESR experiments in the Ni-doped spin-Peierls compound CuGeO_3 ¹⁴. Second, the defects in a spin-gap (and hence, nonmagnetic) matrix can induce the long range antiferromagnetic ordering due to correlation of spins in neighboring clusters. Such an induced antiferromagnetic ordering was observed in the dimerized phase of the spin-Peierls crystal CuGeO_3 ¹⁵ and in the Haldane compound $\text{PbNi}_2\text{V}_2\text{O}_8$ ¹⁶.

The substitution of magnetic ions by other magnetic or nonmagnetic ions in NaV_2O_5 is not yet reported. The only reliable method to embed magnetic defects into this spin-gap crystal is the creation of sodium vacancies¹⁷. Each vacancy causes a 3d-electron shared by two vanadium ions to couple with an oxygen ion, thus making a next-to-defect rung of the vanadium ladder empty (*i.e.* nonmagnetic). This kind of defects should therefore be equivalent to the diamagnetic dilution or cutting the dimerized $S=1/2$ chains. Nevertheless, one should note that two ladder rungs situated next to the sodium vacancy are electrically equivalent which allows the electron to occupy either site or to jump between the rungs.

The present work is devoted to the study of low temperature thermal and magnetic properties of Na-deficient NaV_2O_5 in order to search for long-range magnetic or-

dering stimulated by defects. It is also interesting to compare the behavior of jumping magnetic defects in this kind of a dimerized spin matrix to the behavior of strongly localized defects in a spin-Peierls compound CuGeO_3 . No transition to an ordered phase was found down to a temperature of 0.07 K, however unusual magnetic and thermal properties due to the defects were observed and a model of jumping defects to describe these properties has been developed. The problem of delocalized magnetic defects is suggested for more detailed theoretical investigation. Further experiments to clarify the question are proposed.

II. EXPERIMENT

A. Samples

The sodium deficient single crystals were prepared by the techniques described in Ref. 17. Single crystals of the stoichiometric compound were embedded in a large quantity of the Na-deficient powder and were heated for one week. The resulting content of sodium in the crystals after heating was controlled with accuracy of about 1 % by comparing the results of x-ray and magnetic measurements to those obtained for reference powder samples. The content of sodium in the powder was determined from the molar ratios of the initial reagents.

B. Specific heat

The specific heat of $\text{Na}_x\text{V}_2\text{O}_5$ samples with different sodium deficiencies was measured in the temperature range 0.3 - 8 K. The samples were put onto the holder mounted by thin thermoinsulating wires inside the massive ring equipped by a thermometer. The temperature difference between the holder and the ring was controlled by Au-Fe thermocouple. The current induced by thermoelectric power of the thermocouple was detected by SQUID. The signal from the SQUID was used in a feed back circuit to support the temperature difference equal to zero by heating the ring. Supplying the known power P to the holder with the sample we measured their temperature in real time, thus obtaining the total heat capacity. More detailed description of the installation and the experimental technique including the correction for the parasitic power etc. is given in Ref. 18. The specific heat of a stoichiometric sample was found to be cubic in temperature according to previous measurements¹⁹. The molar heat capacities of the imperfect samples appeared to be much larger in the whole temperature interval. The contribution of the defects to the heat capacity obtained as a difference between the total value of the molar specific heat of several $\text{Na}_x\text{V}_2\text{O}_5$ samples and that of $x=1.00$ sample is shown in Fig. 1. The specific heat of a perfect ($x=1.00$) sample fitted by T^3 -line is also

given as a reference. The defects contribution may be divided into two main components: the low-temperature part remaining non-zero till at least 0.3 K (see Fig. 2) and the high-temperature power-like tail. The temperature dependence above 4 K is approximately quadratic. The low temperature part increases monotonously in the concentration of defects (*i.e.* in $1-x$) while the value of the quadratic part reaches its maximum at $1-x \simeq 0.04$. A test measurement of the specific heat under magnetic field was performed above 4 K. It was found to be field independent up to 7 T with an accuracy of 10%. Even at the largest vacancy concentration no sign of a phase transition into an ordered state was observed, in contrast to similar measurements on diluted CuGeO_3 .

The contribution of defects to the entropy was calculated numerically by taking the integral $E = \int_{0.3}^T \frac{\Delta C_P}{T} dT$. The temperature dependence of this integral divided by the molar entropy of an ensemble of two-level systems is shown in Fig. 3. One should note that the total entropies of the samples with $x=0.96$ and 0.92 are almost the same while the entropy of the $x=0.98$ sample is twice as small. This probably indicates the appearance of some collective state in the system of defects at high deficiency concentrations.

C. Magnetic susceptibility

In order to look at magnetic properties in the low temperature range, we performed a series of magnetization measurements using a SQUID magnetometer equipped with a miniature dilution refrigerator in the temperature range 0.07 - 1.2 K and in magnetic fields up to 8 T. The temperature dependencies of the magnetization at $H \simeq 0.05$ T were obtained for samples with $x=1.00$, 0.98 and 0.90. The corresponding inverse susceptibilities are shown in Fig. 4. The susceptibility of the stoichiometric sample was found to be Curie-like, with the effective concentration of free $S=1/2$ spins being equal to $6 \cdot 10^{-4}$. The small positive Weiss constant $\theta \simeq 0.03$ K corresponds to weak antiferromagnetic interactions between spins. The magnetic defects give rise to an additional Curie-like contribution to the susceptibility which is nevertheless much smaller than that expected for the system of free $S=1/2$ spins with the number equivalent to one half of the concentration of defects. The Weiss constant increases to $\theta \simeq 0.07$ K. The effective concentrations of free $S=1/2$ spins and Curie-Weiss constants of several samples determined by fitting the magnetic susceptibility below 1 K to a Curie law are given in Table 1.

Table 1

$1-x$	θ , mK	Effective concentration
0	30 ± 10	$6 \cdot 10^{-4}$
0.02	70 ± 10	$3.7 \cdot 10^{-3}$
0.1	70 ± 10	$6 \cdot 10^{-3}$

The inverse susceptibility for samples with small $(1-x)$ values deviate from a linear temperature dependence for $T > 1$ K. This seems to indicate that the effective concentration of spins increases with temperature. On the other hand, we cannot rule out that some of the temperature independent part may be due to non-uniformity along the sample holder (no corrections have been made to the present data).

Test magnetization measurements were made for $x = 0.98$ sample by standard Quantum Design SQUID magnetometer in the temperature range 4 - 77 K. The value of Curie constants obtained from data fits at 4 - 15 K corresponds to $(1-x)/2$ concentration of defects which is in agreement with previous results¹⁷.

The field dependence of the magnetization at $T = 0.077$ K was also studied for these samples. Although the temperature dependence of the susceptibility at low temperature is Curie like, the magnetization was found to have a component which does not saturate till $H = 8$ T (see Fig. 5). It should be mentioned that at $T = 0.077$ K the saturating field resulting in 90%-polarization of free $S = 1/2$ spins is equal to 0.17 T.

There was no indication of a phase transition down to 0.077 K in accordance with the specific heat measurements described above.

D. ESR

The sodium deficiency gives rise to an increase in the ESR intensity at low temperature. Imperfect samples of NaV_2O_5 demonstrate the broadening of the ESR line in the temperature range below 3 K (see Fig. 6) in contrast to the constant value of the linewidth in stoichiometric samples¹⁰. The ESR linewidth of magnetic defects caused by Na-vacancies appears to be narrower than that in a perfect sample which proves the different nature of the residual defects in a nominally stoichiometric sample and of the artificial defects in Na-deficient samples.

III. DISCUSSION

As mentioned in the introduction, the sodium deficiency in NaV_2O_5 crystals appears to give rise to a new kind of magnetic defect in spin-gap systems. Unlike the usual nonmagnetic dilution, when impurity ions are fixed in the basic magnetic matrix and all the spins are localized, the absence of a sodium ion leads to the absence of an electron (but not an ion) at a rung of the vanadium ladder. Because the sodium atoms are positioned symmetrically in between two rungs (see Fig. 7) one can see that the resulting unoccupied rung will have two almost equivalent positions. We suggest that this extra degree of freedom for the electron position is very important for the system with exchange interactions and we will try to explain the observed effects starting from this point.

We also assume that the ground state of the electron is localized at one of the two next-to-vacancy rungs. In spite of the obvious loss in energy due to electron localization (of the order of the hopping amplitude³ $t_{\parallel} \sim 0.15$ eV), this assumption seems plausible. Mentioning, that the charge ordering phase transition observed at $T = 36$ K is also followed by localization of electrons (at the ends of the rungs, with the corresponding hopping amplitude $t_{\perp} \sim 0.35$ eV) one can suggest the existence of an additional localization mechanism. For example, the shift of the electron to one of the rungs may break the symmetry of its potential hole in the vicinity of defect, thus strongly diminishing the hopping amplitude.

The most obvious consequence of the sodium (electron) deficiency may be understood neglecting for the exchange alternation. As mentioned above, the diamagnetic dilution of 1D-magnets usually cuts magnetic chains into fixed segments with an equal probability for them to contain an odd or an even number of spins (we shall refer them to as "odd" and "even" segments). However electron jumps can result in a disproportion between them. The ground state energy of a uniform even segment is $E_{\text{even}} = -NE_0 - a/N$ and that of an odd one is $E_{\text{odd}} = -NE_0 + b/N$, where $E_0 \simeq 0.886J$, $b \simeq 2a \simeq 3.5J$ and N is the number of spins in a segment²⁰. Thus, the even states correspond to a gain in exchange energy. A one electron jump between "odd-odd" and "even-even" states of two neighboring segments can change the energy by approximately $\Delta E \sim (a + b)/N$. Naturally, for long chains this effect should be strongly damped by dimerization which, nevertheless gives an additional gain in energy corresponding roughly to the spin gap energy, which comes from the recovering of "dimers" in even segments. It is also reasonable to suggest the existence of a random electrostatic potential in a crystal with defects which makes the neighboring rungs slightly inequivalent. For simplicity one can assume it to be constant but of a random sign $U = \pm\epsilon$. Taking the statistical distribution of segment length N , $f(N) = (1-x)x^N$ ($1-x$ - concentration of chains breaks) we obtain a set of two-level systems with the following molar heat capacity:

$$C = \frac{1}{2}(1-x)N_A \sum f(N) (C(\Delta_N^-) + C(\Delta_N^+)), \quad (1)$$

where $C(\Delta_N^{\pm})$ is the heat capacity of a two-level system with the gap

$\Delta_N^{\pm} = |\Delta E(N) \pm \epsilon|$. This formula describes qualitatively the low temperature part of the experimental curves for various concentrations of defects (see Fig. 1,2).

Consider also the behavior of such a system under magnetic field which splits the energy levels corresponding to the odd states of the chains. One can easily obtain the following formula for the magnetization:

$$M(H, T) = \frac{1}{2}(1-x)\mu N_A \sum f(N) \frac{e^{\frac{\mu H}{kT}} - e^{-\frac{\mu H}{kT}}}{e^{\frac{\mu H}{kT}} + e^{-\frac{\mu H}{kT}} + e^{\frac{\Delta E(N) \pm \epsilon}{kT}}}, \quad (2)$$

where the summation is performed over N for $+\epsilon$ and $-\epsilon$. The result is in surprisingly good agreement with the corresponding experimental data (see Fig 4,5). This effect has a simple interpretation: due to a gain in exchange energy, the number of even segments is initially larger than that of odd ones which is the reason for the system of defects to be almost nonmagnetic in the ground state. The effective number of magnetic objects (odd chains) may increase either by thermal activation or under magnetic field due to a gain in Zeeman energy. (Note, that the small steps at theoretical curves on Fig. 5 result from the discrete distribution of two-level systems by energies $\Delta E(N)$). One must emphasize that this very rough model does not cover the effects of dimerization and correlations between defects and ladders. In addition it implies that the electrons are strongly localized at one of two next-to-vacancy rungs. The aim of this model is only to demonstrate the main features of the thermodynamic behavior of jumping defects.

The observed low temperature widening of the ESR line in Na-deficient samples may result from the freezing out of electrons jumps in the vicinity of defects. When jumps are activated the ESR line should be narrowed by this kind of motion similar to the magnetic resonance line in a liquid.

The unexpected result of the specific heat measurements is the observation of a power-like contribution at relatively high temperatures. While the low temperature part can be described in terms of the thermal activation of local modes (electron jumps) the power-like tail could indicate correlations of some kind between defects which may be of at least two origins.

- a.) The correlation between edge spins in segments due to a gain in exchange energy for "even" chains: The jump of one edge electron of a segment affects the electron at the other edge forcing it to shift in the same direction (for even number of rungs between the vacancies) or in the opposite direction (for odd number) in order to recover the initial parity (see Fig. 7). Thus, the initial jump appears to be a perturbation transmitting along the ladder. These shifts also disturb the zigzag pattern in neighboring ladders because of the correlations between them, which allows this perturbation to transmit also in the transverse direction. One should mention that Fig. 7 shows the perturbations damaging the dimerized state of the segments. It is also possible to imagine a situation where the dimerization is restored in which case it is obviously not the same gain in exchange energy. A detailed theoretical study of the correlations between such defects is required.
- b.) The spin clusters arising around the defect in a dimerized spin-gap matrix: Several spins should be correlated antiferromagnetically in the vicinity of each defect and the interchain interaction may

cause the long-range AFM ordering¹¹⁻¹³. Such an ordering forces each pair of spins separated by an empty site to be parallel, otherwise the interchain interaction appears to be frustrated (see Fig 8). In case of NaV_2O_5 this frustration may be caused by AFM exchange J^* between edge spins appearing due to electron jumps. It is probably the reason for the absence of the spin vacancy induced long range ordering confirmed in the present work down to $T = 0.077$ K. Nevertheless, the defects should induce a frustrated 2D-magnet instead of an antiferromagnet. This is a strongly correlated system (see, for example, Ref. 21) whose specific heat is known to be power-like in temperature as observed in our experiment.

It would be interesting to search for the phase transition into an ordered state in crystals of NaV_2O_5 with a partial substitution of V-ions for other ions (*e.g* for Ti) fixed in the lattice. First, the susceptibility resulting from such a substitution would probably be much larger than those reported in this work. It may also result in the creation of either an ordered state or a frustrated magnet, or a spin glass state. It will thus be very interesting to compare the properties of fixed and jumping defects and their influence on the spin-gap phase of NaV_2O_5 . From the theoretical point of view it is very interesting to study the problem of localization of electrons in the vicinity of unoccupied rungs of the spin ladder (with and without dimerization). The problem of the interaction of jumping electrons with the spin gap matrix has not been studied either.

IV. CONCLUSIONS

The contribution to the specific heat, magnetic susceptibility and ESR signal provided by defects in the spin gap matrix of NaV_2O_5 was observed. The data may be qualitatively described considering the defects as unoccupied rungs of a ladder structure. These defects provide spin and jumping degrees of freedom. The temperature dependence of the specific heat reveals local modes and correlation between defects. We ascribe local modes to electron jumps in the vicinity of unoccupied rungs of the ladder structure. The correlation of defects is explained qualitatively by a model of perturbations caused by electron jumps transferred along the ladder and to the neighboring ladders. Another possible mechanism of the correlation is the generation of magnetic clusters around defects which result in a frustrated 2D-magnet. The absence of an induced long range antiferromagnetic order (in contrast to other spin-gap systems) is interpreted as the consequence of the geometric frustration of the exchange interaction between antiferromagnetic clusters. Magnetic properties of the system of defects are characterized by the temperature dependent effective

spin concentration and by the nonsaturating magnetization curves. These properties are also described in the frame of the jumping defect model.

V. ACKNOWLEDGMENTS

This work was supported by CIES (France), the Russian Fund for Basic Researches grant 98-02-16572 and INTAS grant 99-0155. Authors thank J. Flouquet, D. I. Khomskii, M. V. Mostovoy, A. N. Vasil'ev and M. E. Zhitomirskii for valuable discussions.

-
- ¹ M. Isobe and Y. Ueda, J. Phys. Soc. Jpn. **65**, 1178 (1996).
² P. Horsch and F. Mack, European Physics Journal B **5**, 367 (1998).
³ H. Smolinski, C. Gros, W. Weber, U. Peuchert, G. Roth, M. Weiden, and C. Geibel, Phys. Rev. Lett. **80**, 5164 (1998).
⁴ H. G. von Schnering, Y. Grin, M. Kaupp, M. Somer, R. K. Kremer, O. Jepsen, T. Chatterji, and M. Weiden, Z. Kristallogr. **213**, 246 (1998).
⁵ P. Thalmeier and P. Fulde, Europhysics Letters, Condensed matter **44**, 242 (1998).
⁶ M. V. Mostovoy and D. I. Khomskii, Solid State Commun. **113**, 159 (2000); cond-mat/9806215 (unpublished).
⁷ H. Seo and H. Fukuyama, J. Phys. Soc. Jpn. **67**, 2602 (1998).
⁸ A. I. Smirnov, M. N. Popova, A. B. Sushkov, S. A. Golubchik, D. I. Khomskii, M. V. Mostovoy, A. N. Vasil'ev, M. Isobe and Y. Ueda, Ph.Rev.B **59**, 14546 (1999)
⁹ L. N. Bulaevskii, Fiz. Tverd. Tela **11**, 1132 (1969) [Sov. Phys. Solid. State **11**, 921 (1969)]
¹⁰ A. N. Vasil'ev, A. I. Smirnov, M. Isobe and Y. Ueda, Phys. Rev. B **56**, 5065 (1997)
¹¹ D. I. Khomskii, W. Geertsma and M. V. Mostovoy, Chech. J. Phys. **46 Suppl. S6**, 3239 (1996).
¹² H. Fukuyama, T. Tanimoto and M. Saito, J. Phys. Soc. Jpn. **65**, 1182 (1996).
¹³ Y. Meurdesoif and A. Buzdin, Phys.Rev.B **59**, 11165 (1999).
¹⁴ V. N. Glazkov, A. I. Smirnov, O. A. Petrenko, D. McK. Paul, A. G. Vetkin and R. M. Eremina, J. Phys.: Cond. Matt. **10**, 789 (1998).
¹⁵ L. P. Regnault, J. P. Renard, G. Dhahlenne and A. Revcolevschi Europhys. Lett. **32**, 579 (1995).
¹⁶ Y. Uchiyama, Y. Sasago, I. Tsukada, K. Uchinokura, A. Zheludev, T. Hayashi, N. Miura, and P. Boni, Phys. Rev. Lett **83**, 632 (1999).
¹⁷ M. Isobe and Y. Ueda, Journ. of Alloys and Compounds **262-263**, 180 (1999).
¹⁸ E. Janod, R. Calemczuk, J. Y. Henry and C. Marcenat, Phys. Lett. **A 205**, 105 (1995).

- ¹⁹ D. K. Powel and J. W. Brill, Phys. Rev. B **58**, R2937 (1998).
²⁰ J.C.Bonner and M.E.Fisher, Phys.Rev.**135**, A640 (1964).
²¹ P. Schiffer and A. P. Ramirez, Comments Cond. Mat. Phys. **18**, 21 (1996).

Figure captions

Fig. 1. The contribution to the specific heat from defects at various concentrations. Solid line is the quadratic high temperature approximation, dotted and dashed-dotted lines are calculations by formula (1) with the parameters $\epsilon=7$ K, $a + b=450$ K and 350 K for $x=0.96$ and 0.98 respectively, dashed line is T^3 -fit to the phonon part of the specific heat (perfect sample) subtracted from all the data.

Fig. 2. The residual low temperature part of the contribution to the specific heat from defects. Lines are the same as in Fig. 1.

Fig. 3. The temperature dependence of the molar entropy of the defects.

Fig. 4. The temperature dependence of the inverse susceptibility for samples with various Na-deficiency, $\mathbf{H} \parallel b$. Solid lines are theoretical fits by formula (2) with the parameters $\epsilon=8$ K, $a + b=400$ K and 300 K for $x=0.98$ and 0.90 respectively. Dashed line is the linear fit of low temperature points.

Fig. 5. The field dependence of magnetization at $T = 0.077$ K, $\mathbf{H} \parallel b$. Solid lines are theoretical fits by formula (2) with the parameters as in Fig. 4. Dashed line is the magnetization of a paramagnet with the effective spin concentration $(1 - x)/2$ ($x=0.98$).

Fig. 6. The temperature dependence of the ESR linewidth at $f=36$ GHz, $\mathbf{H} \parallel b$; solid lines are guide-to-eyes.

Fig. 7. Schematic representation of the charge ordered ladder structure in the (ab) -plane of the NaV_2O_5 crystal according to Ref. 6. Solid lines represent the paths of exchange interaction. Vanadium ions are positioned at the intersections of ladder rungs and legs; closed circles are V^{4+} ions, open circles are V^{5+} ions, grey circles are ions with jumping electrons; triangles are the projections of sodium vacancies onto the (ab) -plane. The pairs within dashed ovals are coupled by larger exchange interaction ("dimers"). The arrows show the direction of correlated electron jumps excited at finite temperature.

Fig. 8. An antiferromagnetic interchain frustration due to electron jumps (frustrated region is outlined by dashed rectangle). For simplicity the zig-zag patterns are shown as chains.

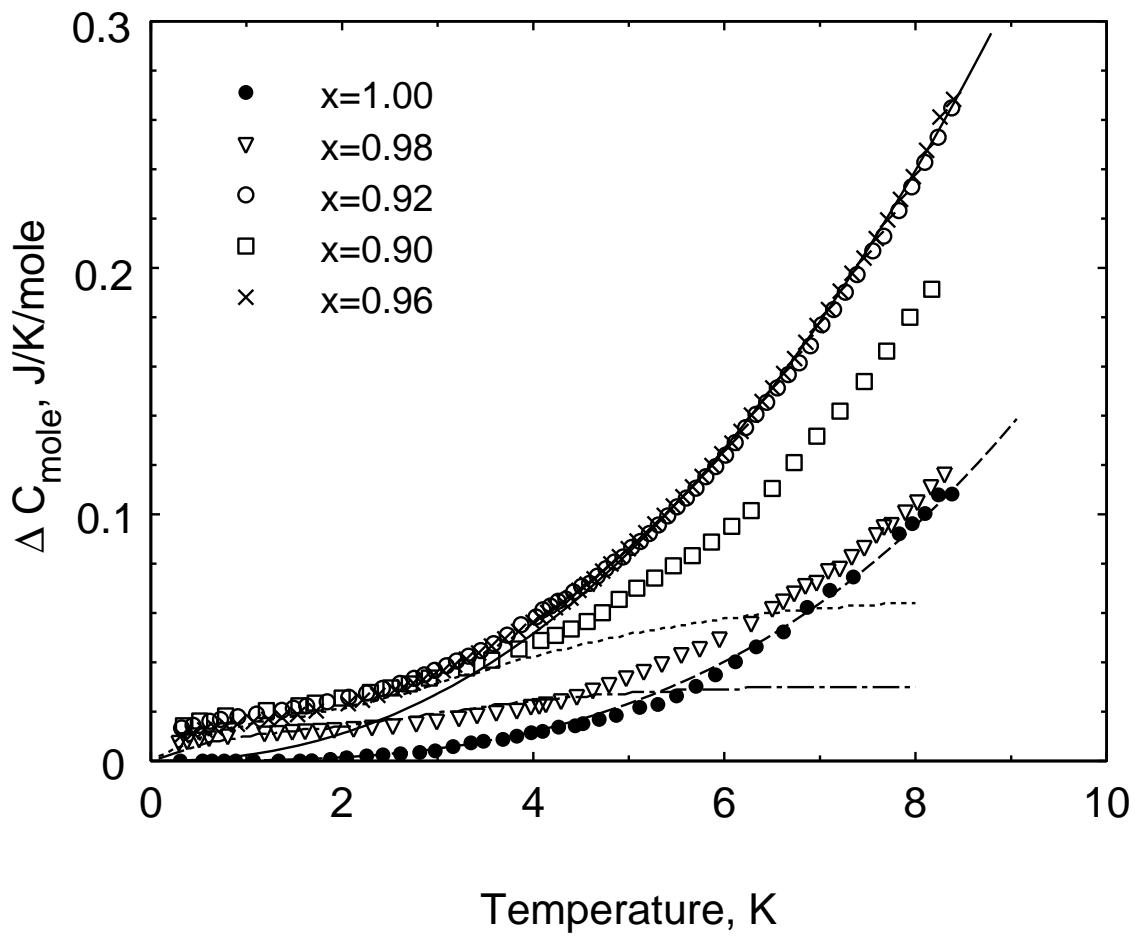


Fig.1. Smirnov et al

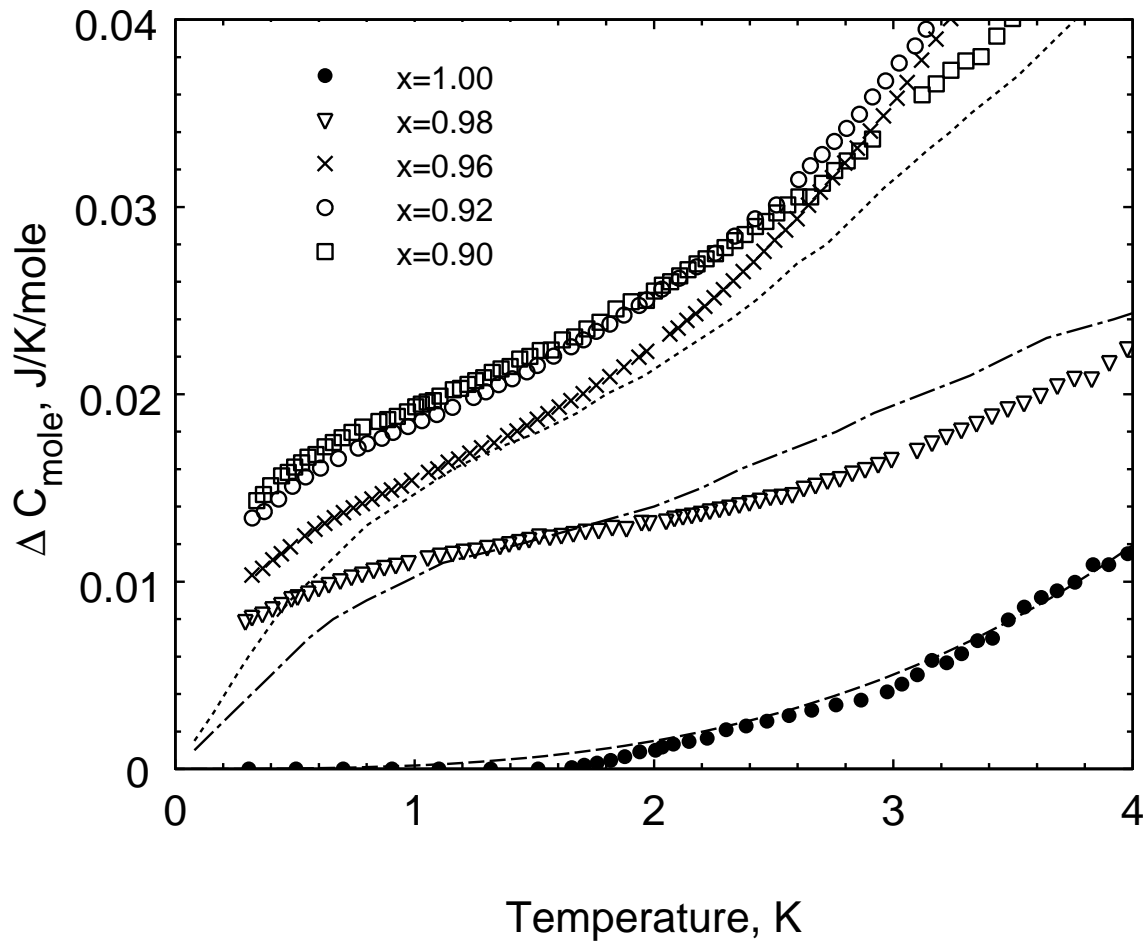


Fig.2 Smirnov et al

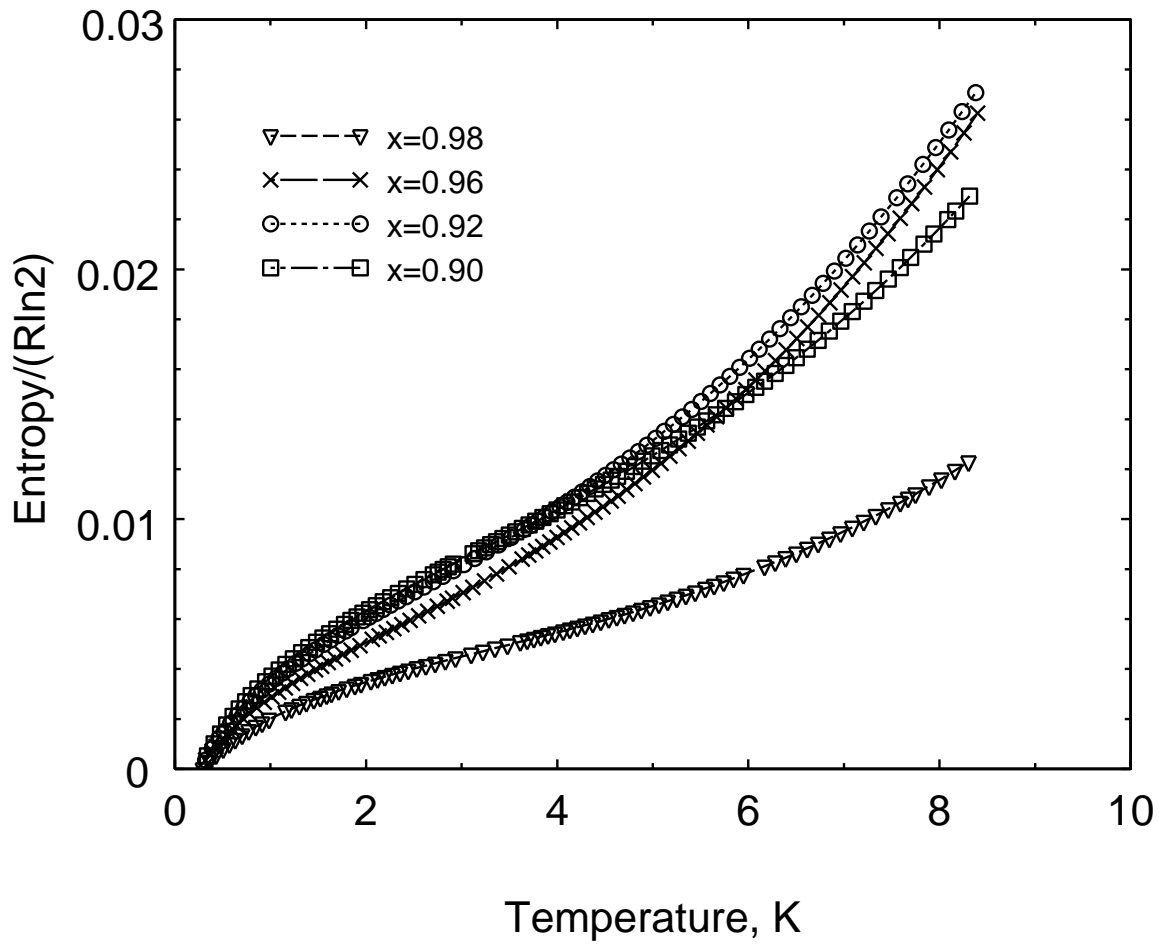


Fig.3 Smirnov et al

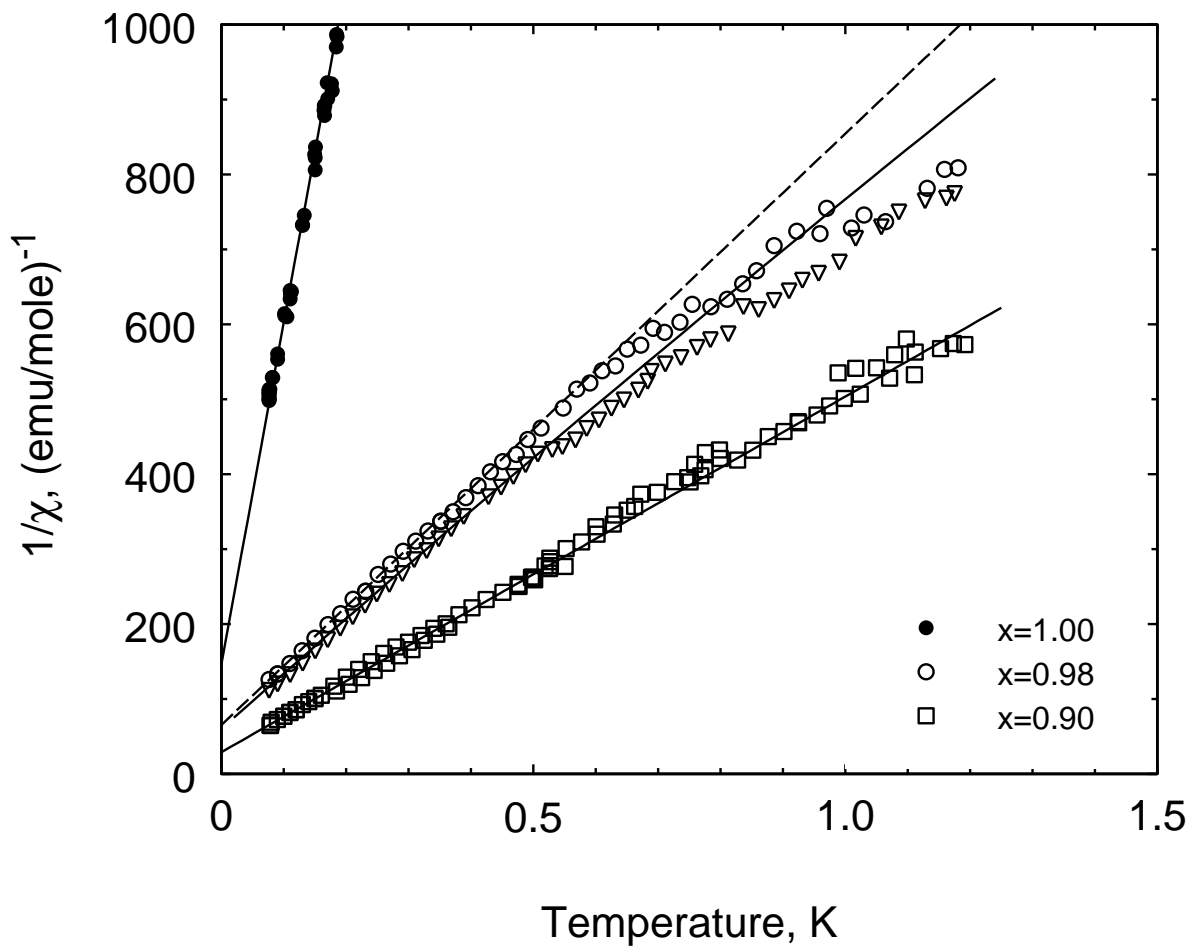


Fig.4 Smirnov et al

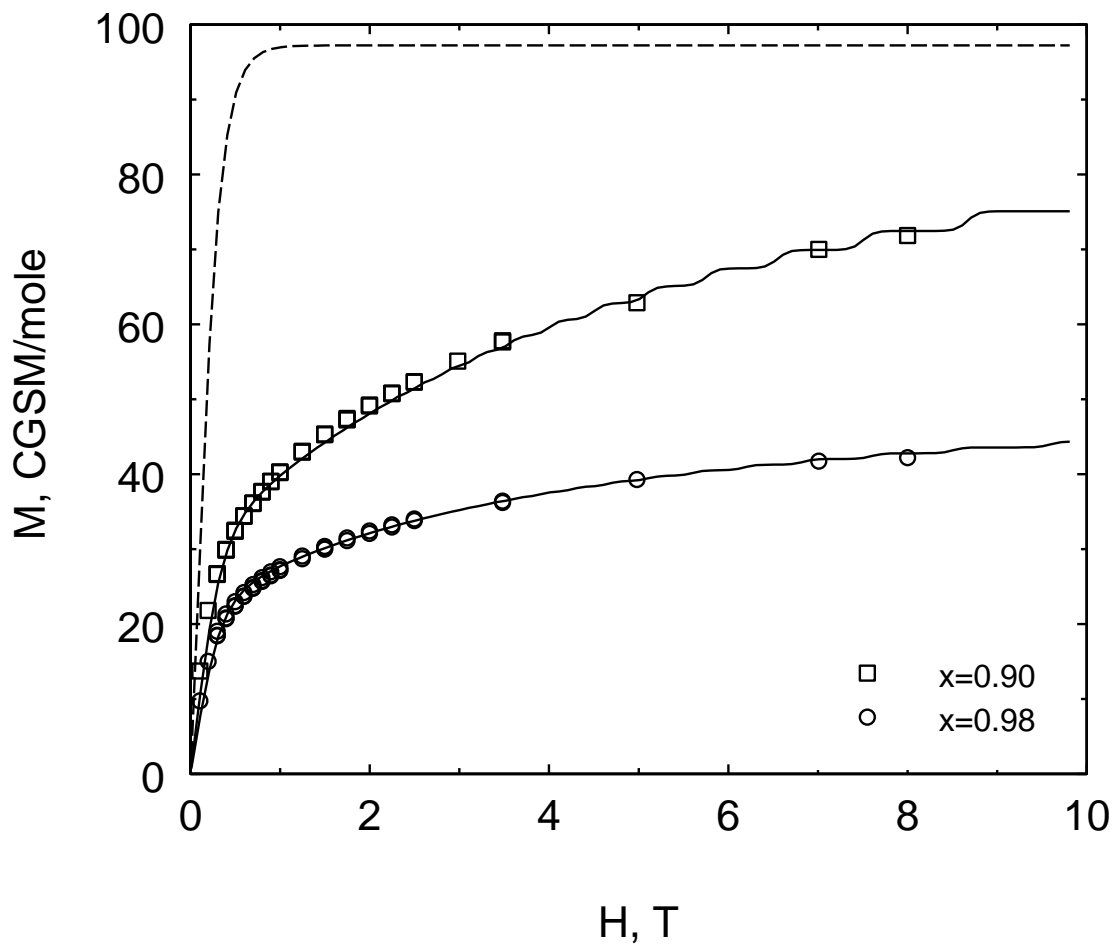


Fig.5 Smirnov et al

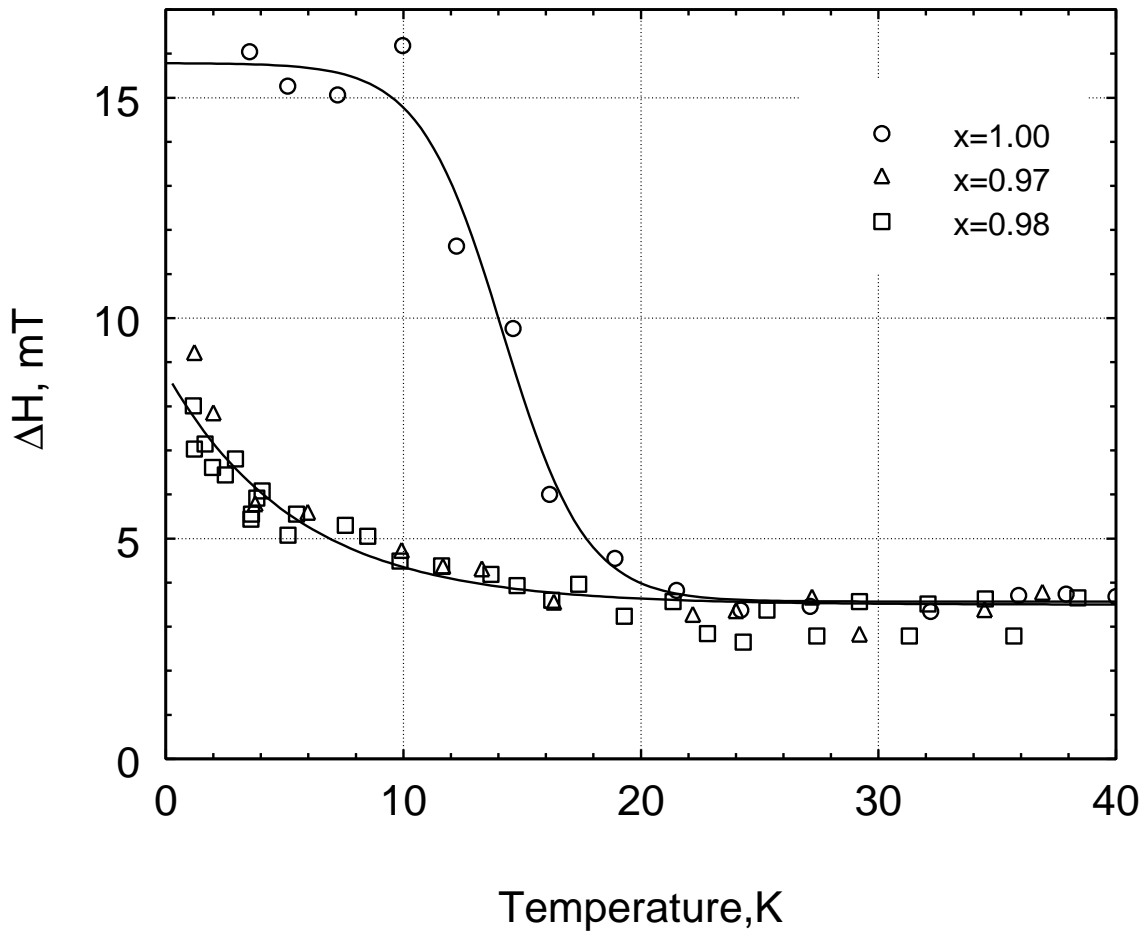


Fig.6 Smirnov et al

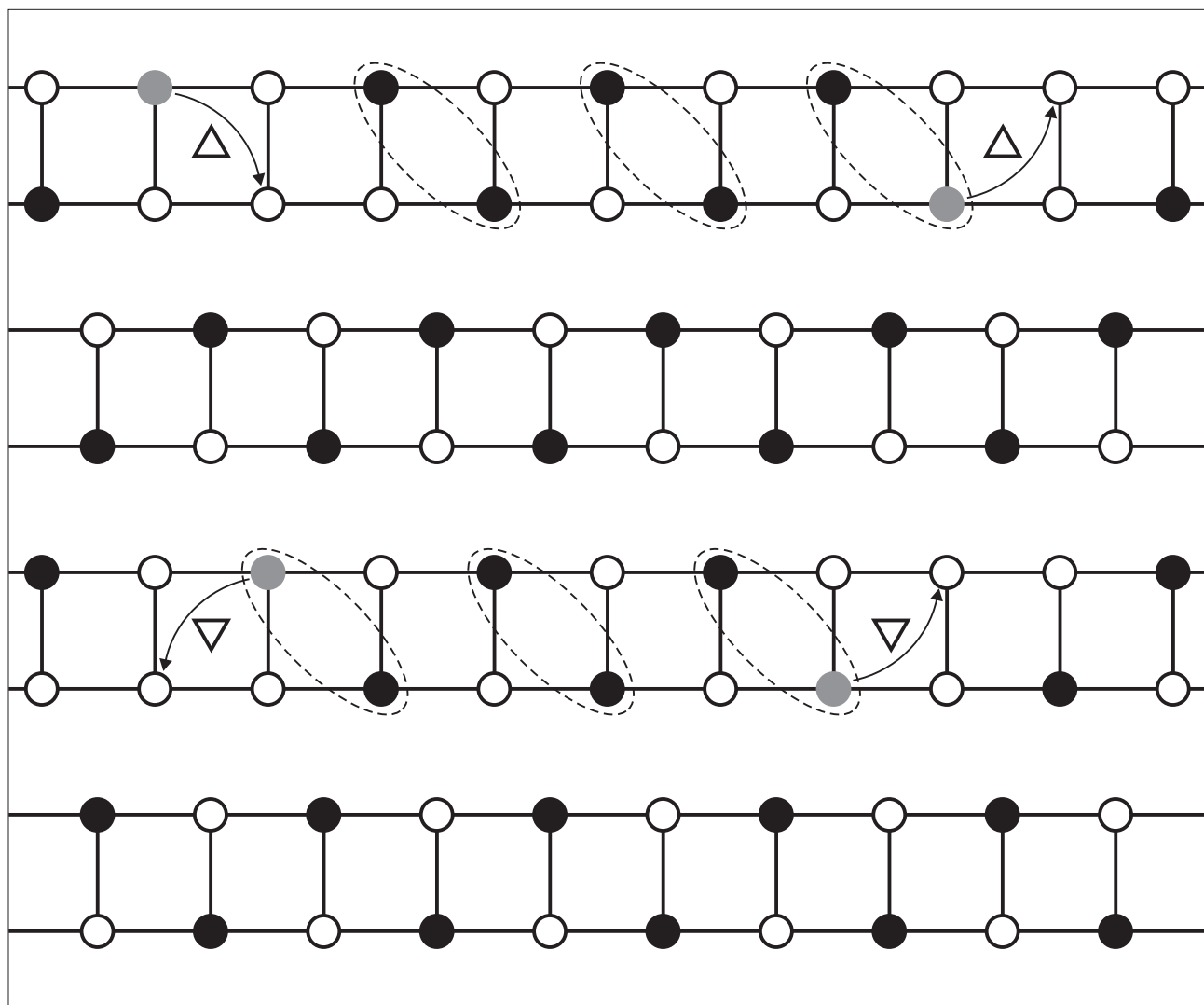


Fig. 7, Smirnov et.al.

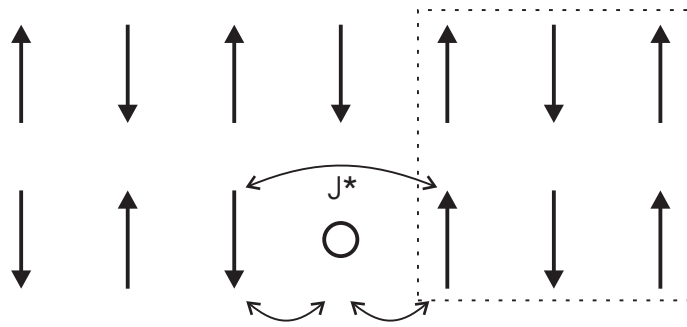


Fig. 8, Smirnov et.al.